Click and Sea: using bioorthogonal click chemistry to visualise seaweed cell walls

Wendy Delpont, Godfrey Neutelings, Zoë A Popper

TECHNICAL ARTICLE

Click & Sea: using bioorthogonal click chemistry to visualise seaweed cell walls

Wendy f. Delpont[1]*, Godfrey Neutelings[2], Zoë a. Popper[1]

[1] Botany and Plant Science, School of Natural Science, College of Science and Engineering, University of Galway, Galway, Ireland, H91 TK33; [2] Univ. Lille, CNRS, UMR 8576 - UGSF - Unité de Glycobiologie Structurale et Fonctionnelle, Lille, France

**For correspondence: wendy.delpont31@gmail.com*

Running title: Click chemistry of seaweed cell walls

Received: 07/01/2025

Returned for revision: 06/05/2025

Editorial decision: 15/05/2025

Keywords: cell wall – seaweed – polysaccharides – bioorthogonal click chemistry – strain-promoted alkyne-azide cycloaddition (SPAAC)

Abstract

- *Objectives*

The study of seaweed cell walls, including their metabolism and composition, is crucial to monitor and understand their adaptation to climate change. Microscopy-based techniques that facilitate studies of seaweed cell walls *in situ*, including staining and immunolabelling, exist but have

significant limitations, including that only a few monoclonal antibodies have been developed towards seaweed cell wall components. Furthermore, not all seaweed cell wall components have been fully described. This makes *in situ* studies focussed on the metabolism of seaweed cell walls particularly challenging. Here, we present a method for labelling seaweed cell walls by incorporating chemical reporters *in muro,* followed by their association with fluorophores by click chemistry.

- *Methods*

Two different species of seaweed, representing different groups, i.e. the red seaweed *Phycodrys rubens* and the green seaweed *Ulva* spp. were selected for their abundance on the Irish coast and because they have relatively thin tissues, a feature likely to facilitate uptake and labelling using monosaccharides reporters. We selected three different activated sugars (fucose, galactose and glucose analogues) on the basis that they are major components of seaweed polysaccharides. Small sections of the seaweeds were incubated with the activated sugars, and their uptake and incorporation were visualised by attachment to the fluorescent probe AF488 and imaged using confocal microscopy.

- *Results*

After incubation with the activated sugars, the seaweed cell walls, i.e. the contours of the cells, and, to a lesser extent, some cell organelles, fluoresced at 517 nm (emission wavelength of AF488), suggesting that the seaweed had incorporated the activated sugars. Fiji software was used to remove nonspecific fluorescence (autofluorescence of the seaweed and non-specific binding of the fluorochrome), with the final images suggesting good and specific incorporation of the fluorochrome by the seaweeds. More interestingly, the fluorescence was primarily associated with

the cell walls, implying that the activated sugars were predominantly incorporated into cell wall components (most likely either polysaccharides or glycoproteins).

- *Conclusion*

To date, bioorthogonal click chemistry has not been applied to seaweed but represents a useful tool for phycologists to better understand seaweed cell wall composition and dynamics, for example, throughout the seaweed life cycle or in the face of stresses (biotic or abiotic), including those resulting from climate change.

INTRODUCTION

The ability to look inside living tissue, specifically inside cells, has always intrigued researchers and has long been a subject of study. However, it can be difficult to recognise and differentiate the cell components. Increasingly sophisticated methods have been developed over the years, enabling the identification of specific molecules: from histological tissue staining in the 1770s (Alturkistani et al., 2016) to immunofluorescence targeting specific parts of polysaccharides and proteins (Coons et al., 1941) to protein labelling via genetics (Chalfie et al., 1994), and, more recently, the integration of fluorescent tags into the genome via genome editing (Schwinn et al., 2018).

Seaweeds are predominantly marine photosynthetic organisms. They are multicellular organisms typically occurring in coastal locations and organised into rock-fixed thalli, although some, such as *Sargassum,* may be pelagic. Some seaweeds can be very small, couple of cm, while can be up to 70 meters long. However, despite similarities, including habitat, multicellularity, and the ability to photosynthesise and produce sulphated polysaccharides, seaweeds are not a single group but rather include several lineages. Seaweeds are enormously diverse and possess many distinct

features. However, they are frequently grouped according to their pigmentation into one of three taxa: green (Chlorophyta), red (Rhodophyta) and brown (Phaeophyceae). In this manuscript, we will focus on their cell wall compositions, a feature that is sufficiently diverse that it has been used as an important character to define individual taxa (Stace, 1989). The green seaweed cell wall is mainly composed of cellulose microfibrils (made up of D-glucose residues), making up 15–30% of the total dry weight of the seaweed (Wahlström et al., 2020). Hemicellulose structures, which play a cohesive role in the wall, are also found. The main hemicelluloses present in green seaweed are xyloglucans, mannans and β-(1-3)-glucans. Other polysaccharides, called ulvans, are found only in the Chlorophyta. Ulvans are sulphated polysaccharides composed mainly of L-rhamnose and glucuronate chains to which D-xylose, iduronic acid, D-mannose, D-galactose and fucose residues may be added. Ulvans are made up of a disaccharide repeat, whose composition can vary. However, there are two main combinations of repeats: type A and type B. Type A is called ulvanobiuronic acid 3-sulphate (A3S) and is made up of rhamnose-3-sulphate and glucuronic acid or iduronic acid. Type B is called ulvanobiuronic acid 3-sulphate (B3S) and is made up of rhamnose-3-sulphate and xylose (Lahaye & Robic, 2007). Carbohydrates are stored as starch in green seaweed, like in land plants. This starch is formed of two polymers, amylose and amylopectin, composed of D-anhydroglucopyranose (Prabhu et al., 2019).

Other molecules, such as glycoproteins, including arabinogalactan proteins (AGPs) and extensins, are also present in the cell walls of green seaweed. AGPs and extensins also occur in green land plants (Clarke et al., 1979). However, green seaweed AGPs and extensins have structural features that are seaweed-specific, such as a unique sugar residue profile and the presence of sulfated sugars that are not present in most land plants (Estevez et al., 2009; Liu et al., 2016; Přerovská et al., 2021).

In red seaweed cell walls, cellulose microfibrils constitute only 1–10% of the total dry weight of the seaweed (Ross, 1953) and may be replaced by either glucomannans or xylans, depending on the species. Similarly to ulvans in the Chlorophyta (green seaweed), red seaweed possesses specific polysaccharides, carrageenans and agars. Carrageenans are linear sulphated galactans composed of repeat units of α-D-galactopyranose and β-D-galactopyranose residues. There are fifteen different types of carrageenans known based on their degree of sulfation and the location of sulfate side groups. Nevertheless, only three carrageenans are commonly found: the ι- (iota), κ- (kappa) and λ- (lambda) carrageenans (Lahaye, 2001; Stiger-Pouvreau et al., 2016). Agar is composed of two different types of molecules called agarose and agaropectin. Both molecules are made up of disaccharide repeat units composed of-D-galactopyranose and anhydro-3,6-α-L-galactopyranose (Usov, 2011). Agarose is a linear polysaccharide, and agaropectin is a branched polysaccharide. Some sulphate groups may be attached to the agaropectin structure, which confers a degree of sulfation to the molecule (Lahaye & Rochas, 1991). Red seaweed also stores carbohydrates in the form of starch. However, this starch is different to the starch found in green seaweed and land plants and is called floridean starch. Although floridean starch is composed of a highly branched succession of α-(1→4) linked glucose units, (Ball et al., 2011) it differs from the starch found in land plants by its composition and degree of branching.

Seaweed cell walls, similarly to those of land plants, play important roles in cell structure, cell growth and the maintenance of cell homeostasis. The cell wall is also a physical barrier involved in interacting with the environment and its various stresses and in cell-cell communication (Kloareg & Quatrano, 1988; Popper et al., 2011). As a result, their cell wall compositions are diverse (Table 1), and many seaweed are commercially important, predominantly because of their constituent polysaccharides that are largely used for their gelling and viscosifying properties in

biomedical, pharmaceutical, cosmetic (Cardozo et al., 2007; Pereira, 2018), food and feed, agricultural (Craigie, 2011), textiles (Lomartire et al., 2022) industries as well as for biofuels (Sharmila et al., 2021) and bioremediation (Ibrahim, 2011; Leandro et al., 2020; Makkar et al., 2016; Ścieszka & Klewicka, 2019). In 2023, the market for seaweed products was valued at 5.3 billion USD, and forecasts predict an average annual growth of 6.4% to reach a total market of 7.3 billion USD by 2028 (MarketandMarkets, 2023). Although used in a wide range of fields and carrying considerable weight in the world markets, the components and dynamics of seaweed cell walls are not well studied *in situ*.

Different techniques have been developed to study the cell walls and their components in seaweed. Specific histological stains, including alcian blue, calcofluor white or concanavalin A, can be used to observe and follow the metabolism of cell wall components. For example, Martone et al., in 2010, observed the growth of the red seaweed *Calliarthron cheilosporioides* using calcofluor white (Martone, 2010). Other techniques, such as immunolabeling and the development of specific monoclonal antibodies, for example, to different alginate structures, have allowed researchers to look at the development of zygotes in the brown seaweed *Fucus* (Torode et al., 2016).

Despite the progress made in understanding seaweeds using these methods, there are many limitations, including that seaweed cell walls are highly diverse and that their components, even some of those that are amongst the most widely used, such as fucoidans, have not yet been fully characterised. A few monoclonal antibodies that were developed against land plant cell wall components can recognise features present in brown (Raimundo et al., 2016) and green seaweeds (Estevez et al. 2009; Fernández et al. 2010). However, the development of highly specific monoclonal antibodies that label structures present in seaweed cell wall polysaccharides, giving insight into their location and metabolism, has been very limited. This is especially the case in

comparison to the large array of different monoclonal antibodies available against plant cell wall components (Duffieux et al., 2020; Pattathil et al., 2010). Currently, only a few monoclonal antibodies are available that were specifically developed against seaweed cell wall components. These include the range of monoclonal antibodies, commercially available from SeaProbes (https://www.sb-roscoff.fr/en/seaprobes), that recognise and bind to alginates and fucoidans found in brown seaweed (Torode et al., 2015, 2016). These antibodies recognise alginates with different sulfation levels and possess different ratios of glucuronic and mannuronic acids (Torode et al., 2015, 2016) and have enabled improved knowledge of zygote development in brown seaweed (Torode et al., 2015, 2016). Monoclonal antibodies have also been made to ulvans (Rydahl et al., 2017). Many more seaweed cell wall polysaccharide-specific monoclonal antibodies were developed, predominantly to brown seaweed polysaccharides (Jones et al., 1988; Vreeland, 1970; Vreeland & Laetsch, 1989) but also to carrageenans from red seaweeds (Vreeland et al., 1992). Unfortunately, the majority of these antibodies are no longer commercially available to the scientific community (Raimundo et al., 2016), and information regarding the localisation and dynamics of seaweed cell wall polysaccharides, despite increasing in recent years (Estevez et al. 2009; Fernández et al. 2010, Torode et al., 2015, 2016, Raimundo et al., 2015, 2026), remains scarce (Raimundo et al., 2016), particularly for red seaweeds.

Red seaweed cell walls, despite the significant commercial importance of their polysaccharides, are comparatively less well characterised than green and brown seaweed cell walls, and there remains a distinct lack of available tools for studying their *in situ* dynamics, e.g., in response to climate change.

In the 1960s, Huisgen (Huisgen, 1961) developed the concept of 1,3-dipolar cycloadditions, which highly inspired K. B. Sharpless, who first used the term “click chemistry” (Kolb et al., 2001). His

laboratory and that of Morten Meldal have developed copper-catalyzed regioselective chemical associations of the Huisgen cycloaddition of azides and terminal alkynes to form 1,2,3-triazoles. They were awarded the Nobel Prize in Chemistry in 2022, along with Carolyn Bertozzi, who, in the late 1990s, described the possibility of carrying out such reactions under biological conditions inside cells. These reactions are called bioorthogonal, meaning they occur rapidly in aqueous solutions, in the presence of biological molecules, at low concentrations, and are extremely selective, as they only react with a single functional group. The reactions resulting from these works are azide-alkyne cycloadditions depending (CuAAC: copper-catalysed azide-alkyne cycloaddition) or not (SPAAC: Strain Promoted Alkyne-Azide Cycloaddition) on copper. In the first case, the copper(I) ion lowers the activation energy, making the reaction highly efficient and selective, and in the second case, the strain in the cyclooctyne drives the reaction with the azide, bypassing the need for copper (Agard et al., 2004). The use of click chemistry approaches is generally straightforward from a technical point of view, with the only possible difficulties being the mobility of reporters across cell interfaces and verification of their compatibility with cellular metabolism. The real challenge, however, remains their synthesis when they are not commercially available, as is the case for lignin precursors (Morel et al., 2022).

Although CuAAC and SPAAC have been successfully applied to study plant cell walls (Anderson et al., 2012; Lion et al., 2017; Morel et al., 2022; Simon et al., 2018), it appears not to have been applied to seaweed cell walls. In this article, we adapted and applied the SPAAC technique to seaweed to label their cell wall components. The seaweed species were chosen because of their availability on the Irish coast so that the material used could be as fresh (and as metabolically active) as possible and for the thinness of their tissues, which typically is associated with better uptake and integration of the reagents used in the click chemistry reactions. The green seaweed,

Ulva, was additionally chosen as it has been sequenced (De Clerck et al., 2018), and its cell wall components are relatively well-characterised (Bothwell et al., 2022; Lahaye & Robic, 2007). The red seaweed, *Chondrus crispus*, has also been sequenced (Collén et al., 2013) and has commercial importance in part derived from its high concentration of carrageenans. The gametophyte and sporophyte can also be distinguished since the gametophyte generation exhibits autofluorescence (Fournet et al., 1993).

To the best of our knowledge, click chemistry has not previously been applied to seaweed. We tested the integration of three modified sugar residues that commonly occur in cell wall components (fucose, galactose, glucose). We were then able to observe the cell components that had integrated the modified sugar residues by reacting them to attach a fluorescent dye and visualising using confocal microscopy.

METHODS

Collection of seaweed

Seaweeds were collected at low tide in May 2023 at An Spidéal, Co. Galway, Ireland (53°14' 33" N – 9°18'23" W). This collection site is predominantly sandy, surrounded by sandstone rocks in which there are intertidal pools at low tide.

Two species of seaweed were collected: one red seaweed (*Rhodophyta*), *Phycodrys rubens,* and one green seaweed (*Chlorophyta*) *Ulva spp* (Fig.1). All the seaweeds collected were visually ungrazed or damaged, adult in appearance, and clean with no visible parasites.

After collection, the seaweed samples were transported to the laboratory in a sealed plastic bag containing seawater. In the laboratory, the samples were washed using clean seawater to remove

any particles of sand and placed into 50 mL Falcon tubes containing clean seawater. The samples were stored at 10°C for approximately 20 hours, followed by storage at 4°C for 40 hours. The seaweed samples were then cut into small square sections (approximately 20 mm by 20 mm) using dissecting scissors.

Sugar reporters

The ability of the seaweed sections to uptake and incorporate three common monosaccharide reporters was tested. The monosaccharide reporters were 1,2,3,4-Tetra-*O*-acetyl-6-azido-L-fucopyranose (TF608, Synthose, Concord, Canada), 1,3,4,6-Tetra-*O*-acetyl-2-azido-2-deoxy-D-galactopyranose (TL709, Synthose, Concord, Canada), and 1,3,4,6-Tetra-*O*-acetyl-2-azido-2-deoxy-D-glucopyranose (TG713, Synthose, Concord, Canada) (Fig.2). These three modified monosaccharides contain an azide moiety, which allows another molecule, previously linked by an alkyl moiety, to attach to them together and form a triazole. In addition, the peracetylated forms were chosen to allow transport inside the cells (Anderson & Wallace, 2012).

Fluorochrome

For the modified sugars to bind to an azide group, a molecule containing an alkyl group must be present. To visualise the modified sugars, they must be linked to a probe that can be seen under the microscope. Fluorescent probes have typically been used for click chemistry (Mbua et al., 2011; Simon et al., 2018; Subramanian et al., 2014). The DBCO-AF488 (dibenzocyclooctyne bound to the fluorescent probe AF488) was used in this study (Fig.3). We chose to use AF488 to avoid interference from strong autofluorescence. Autofluorescence from seaweed would, most likely, be derived from chlorophyll a. Therefore, the selection of the fluorescent probe AF488 limits autofluorescence from chlorophyll a since AF488 emits at a wavelength of 517 nm, i.e. in

the green part of the spectrum, whereas chlorophyll a emits between 685–690 nm, in the red part of the spectrum.

Reporter integration

The experimental protocol is summarised in Figure 4. Three fragments of each seaweed species were placed in the wells of 24-well microplates with 500 µL of 1X PBS (Phosphate-buffered saline) solution. The seaweed sections were incubated in 300 µL of 10 mM of the reporter solution at room temperature, under agitation at 300 rpm for either 24- or 48 hours. Two controls were carried out: (1) to determine autofluorescence of seaweed cell components using confocal microscopy (no reporter, no fluorochrome) and (2) non-specific binding of the fluorochrome (no reporter, + fluorochrome).

Fluorochrome integration

After either 24- or 48 hours, the reporter solution was removed, and the seaweed sections were washed three times using 500 µL of 1X PBS solution. The sections were then incubated at room temperature, in the dark, in a 5 µM DCBO-AF488 (Jena Bioscience, Jena, Germany) solution for 90 minutes, with 300 rpm agitation (Thermo-Shaker, PHMP-4). After the addition of the probe, all the following steps were carried out in the dark to limit the degradation of the probe.

Tissue washing

Tissue washing was carried out by incubating the sections in methanol 70% v/v for 1 hour, in the dark, with 300 rpm agitation, in the dark. This step aimed to remove the fluorophores non-

specifically bound to the cells and fix the cells to allow better observation. The samples were washed three times with 500 µL of 1X PBS solution.

Confocal microscopy

Before observation, the samples were placed in a drop of Fluoromount-G® (Thermo Fisher Scientific) between a slide and a coverslip and observed using a confocal microscope ZEISS LSM 740. The excitation and emission wavelengths for Alexa Fluor® 488-Azide were 494 and 517 nm, respectively. Microscope settings (gain, laser intensity, pinhole size) were kept constant throughout a given set of experiments to adjust all images in the same way and achieve comparable visualisation of image fluorescence intensities. The images were captured and then analysed and processed using the Fiji software (Schindelin et al., 2012). Each measurement was performed on three independent fragments.

Supplementary Analysis: Validation of Seaweed Cell Components

To better understand and provide additional analytical insights into the images obtained through click chemistry, particularly regarding the intracellular structure of seaweed, iodine and Toluidine Blue O (TBO) staining were performed following the observation of the click chemistry images. *Ulva spp* and *Phycodrys rubens* were collected on November 15th, 2024, at An Spidéal (Co. Galway, Ireland).

Iodine staining

Iodine staining (or Lugol test) was performed on plant cells to localise starch. However, cell wall polysaccharides such as xyloglucans (Yuguchi et al., 2005), carrageenans (which stain pale purple), and agars (Flint, 1990) can also be stained. No publications report the staining of ulvan by the Lugol test. However, xyloglucan is present in the cell walls of green seaweeds, which suggests that their cell walls may be stained by the Lugol test (Wahlström et al., 2020).

Iodine staining is made possible by binding iodine and potassium iodide within sugar chains, specifically within the amylose helices of starch (Minick et al., 1991). To carry out iodine staining, *Ulva spp.* and *Phycodrys rubens* sections were incubated with one drop of Lugol solution (Sigma Aldrich). Following staining, the seaweed tissues were mounted on a microscope slide and covered with a coverslip prior to observation under a light microscope (Optika B-293 and camera Optika C-P6).

TBO staining

Toluidine Blue O (TBO) staining was performed to visualise the cell walls, chloroplasts, and starch. The TBO staining method highlights acidic components in cells and tissues. TBO binds specifically to acidic groups, such as sulfates, carboxylates, and phosphates, that are commonly found in polysaccharides, nucleic acids, and glycoproteins (O'Brien et al., 1964). To perform TBO staining, 0.05% toluidine blue O powder was dissolved in 50 mM sodium acetate buffer (pH 5). A drop of the staining solution was applied to the seaweed tissue and incubated for 2 minutes at room temperature. The tissue was then rinsed with distilled water and mounted between a slide and coverslip for microscopic observation (Optika B-293 and camera Optika C-P6).

RESULTS

Effects of incubation time on labelling intensities

No specific protocols have been previously established for chemical reporter detection in seaweed. We, therefore, incubated fragments of *Ulva spp* and *Phycodrys rubens* in 10 µM N_3-reporters for 24 and 48 h without any permeabilising agent to estimate the optimal time for incorporation. The overall results are summarised in Table 2. For *Ulva*, the 48-hour incubation suggests that the longer the incubation, the greater the signal (Fig.5). This is particularly correlated with more distinct labelling of the cell walls. In *Phycodrys*, the signal intensity also increased over time, but in the case of fucose, the signal intensity within the cell wall remained low at 24 and 48 h (Fig.7, image of 24-hour reporter incubation available in supplementary figures 1–2).

Incorporation of monosaccharide reporters in Ulva spp

A first control lacking both reporters and probes (R-F-) shows a total absence of signal in the thallus, indicating that there is no or undetectable autofluorescence of pigments or other cellular components at excitation/emission wavelengths of DCBO AF 488 (Fig.5a, f, k). A second control incubated only with the fluorophore (R-F+) exhibited a very weak fluorescent signal (Fig.5b, g, l). This suggests that there is no strong non-specific binding of the probes

The signal observed with the fucose reporter (fucose, F+) is intense (Fig.5c, h, m) but does not appear to be uniform in all the cells (x20) compared to glucose labelling (Glucose, R+F+), which appears to be more regular (Fig.5e, j, o). The signal derived from the galactose reporter (Galactose, R+F+) is visible in most of the seaweed cells and is more easily visualised at higher magnifications (Fig.5i) magnification x63 and magnification x63x3 (Fig.5n). Signals observed at high

magnification reveals a strong signal for all the reporters at the level of the cell walls but also the inter-cell level.

It was possible to quantify and compare the signals obtained with the three reporters since, in each case, the same bioorthogonal click chemistry reaction occurred between an azide group on the reporter and DBCO anchored on the AF488 fluorophore. In addition, all the settings on the confocal microscope were conserved between each sample. Values were obtained by subtracting the background from the signal.

Quantification was carried out on the cell walls and the internal space of the cells (Fig. 6). For *Ulva* spp., significant differences in incorporation levels were observed, with a higher rate for glucose, followed by fucose, and finally galactose in the cell wall.

Incorporation of monosaccharide reporters in Phycodrys rubens

Using the (R-F-) control, it was possible to exclude the presence of autofluorescence in the *Phycodrys* samples (Fig 7a, f, k). In contrast to the *Ulva* samples, however, we were able to observe the presence of aspecific fluorescence deriving from the presence of residual probes in the tissue as suggested by the (R-F+) control (Fig 7b, g, l). In the (R+F+) samples, the signal intensities were much higher (Fig.7 c, d, e, h, I, j, m, n, o). This suggests that the seaweed can specifically take up and incorporate the reporters. Each of the three different monosaccharides were located in the internal part of the cells, and, as for *Ulva* spp, it was interesting to observe the presence of clear labelling on the cell walls (Fig.7m, n, o). In both compartments, the incorporation measured for glucose was the highest among the three reporters tested (Fig. 6). The comparison between galactose and fucose showed a higher signal for the first in the cell wall and the second inside the cells.

Light microscopy of the intracellular structure of Ulva spp.

Following the staining of *Ulva* spp. with Lugol's solution, numerous black-staining spots of ~1–3 µm in diameter were observed (arrow number 1, Fig. 8e). On average, around seven of these black-staining spots were present in each cell. Additionally, larger spots, ~10-15 µm in diameter, surrounded by a brown-staining membrane, are visible (arrow number 2, Fig. 8e). The cell walls are also visible and were stained light brown (Fig. 8e).

TBO staining was also carried out on *Ulva*. The cell walls are stained pink/purple (Fig. 8f), indicating that they consist predominantly of polysaccharides. Additionally, structures with distinct contours were observed inside the cells (Fig. 8f) and are likely to be cell organelles, including the vacuole, nucleus, mitochondria, and peroxisome (Blomme et al., 2020).

Light microscopy of the intracellular structure of Phycodrys rubens

Iodine staining (Lugol test) is known to stain floridean starch grains (Yu et al., 2021). Iodine staining of *Phycodrys rubens* resulted in dark-staining spots of ~5-10 µm in diameter at the periphery of each cell in the stained tissue (arrow number 1, Fig. 9e). There were approximately three brown-staining spots present in each cell. We also observed the presence of oval structures (5 µm long and 15 µm wide) that were lightly stained brown with the Lugol's stain (arrow number 3, Fig. 9e). There, therefore, appear to be at least two distinct populations of cell organelles that stain with iodine in *Phycodrys*: 1) smaller, dark brown staining, and 2) larger organelles that are more lightly stained (arrow number 3, Fig. 9e). Another structure is more clearly observed

following iodine staining, arrow number 4, and appears to be a connexion between two cells (Fig. 9f).

We also attempted to stain *Phycodrys* sections with toluidine blue O stain to visualise the cell walls, chloroplasts, and starch. However, the red pigment, primarily phycobiliprotein, in *Phycodrys* masked any TBO-staining, and as a result, it was impossible to observe any distinct intracellular staining. In contrast, *Phycodrys* cell walls were stained blue-green and could be clearly visualised (Fig. 9f).

DISCUSSION

Using bioorthogonal click chemistry to monitor the production of cell wall components

We have explored the use of the bioorthogonal click chemistry in two species of seaweeds (from the Chlorophyta and Rhodophyta phyla) by testing the metabolic incorporation of three different modified sugars with the primary objective of incorporating them into cell wall polymers. Plant cell walls contain mainly polysaccharides, and when a secondary cell wall is present, also lignin. Each polymer is synthesised by enzymes located in different compartments, which can make the incorporation of chemical reporters more or less difficult. Lignin precursors, namely *p*-coumaryl alcohol, coniferyl alcohol and sinapyl alcohol, are synthesised in the cytoplasm and transported to the cell wall, where peroxidases and laccases oxidise them before being incorporated into the growing polymer (Zhao et al., 2013). To hijack these natural monomers, an exogenous supply of tagged surrogates on plant sections, meaning directly on the cell wall is sufficient to induce the incorporation (Morel et al., 2022). Concerning polysaccharides, metabolic labelling using sugar analogues compatible with click chemistry makes it necessary to set up conditions such that the

reporters will enter the living cells through the cell wall and plasma membrane and then integrate the synthetic machinery in the Golgi apparatus level for pectins and hemicelluloses or be activated in the cytoplasm for cellulose synthesis. This was first reported by the use of an alkynylated fucose analogue, which was successfully incorporated into the pectic rhamnogalacturonan-I (RG-I) within the cell walls of *Arabidopsis thaliana* roots (Anderson et al., 2012). Rhamnogalacturonan-II (RG-II) labelling in this same organ but also in tobacco (*Nicotiana tabacum* L. cv Bright Yellow-2) cell suspension cultures was also demonstrated later on by using 8-azido-3-deoxy-D-manno-oct-2-ulosonic acid, an azido derivative of Kdo (Kdo-N3) (Dumont et al., 2016). Kdo-N3 was also later incorporated into fast-growing, tip-polarized expanding pollen tubes (Ropitaux et al., 2022). Studies using click chemistry approaches have been carried out on microalgae in very specific contexts. CuAAC click chemistry associated with LC-MS was used to detect polyether toxins (prymnesins) produced by *Prymnesium parvum,* which is associated with harmful seaweed blooms (Hems et al., 2018). Other works have led to the production of microalgae-based microrobot functionalised by click chemistry with angiotensin-converting enzyme 2 (ACE2) receptor against the SARS-CoV-2 spike protein (Zhang et al., 2021). But to the best of our knowledge, the bioorthogonal click chemistry technique has never been reported in seaweed in the context of understanding biological mechanisms.

Tracking analogues of monosaccharides in green and red seaweeds using a bioorthogonal click chemistry approach

Ulva spp, commonly known as sea lettuce, is an excellent model organism for studying green seaweed because of its simple and versatile life cycle and is a major component of marine food networks. It can form seaweed blooms (*e.g.*, green tides) in response to nutrient pollution,

providing a model to study eutrophication. It also exhibits high morphological plasticity, responding to environmental cues by altering its shape and structure (Wichard et al., 2015). Galactose, fucose and glucose, tagged with azide groups, were detected after their association with a fluorescent probe by click chemistry. As described in the higher plant models, the peracetylated forms were able to cross the plasma membrane and were detected in different sub-cellular locations.

The strong labelling observed in the cell wall with the glucose reporter can be explained by the presence of (1) cellulose and (2) ulvans (structure detail in the introduction) within the cell wall of Ulva. Both of these polymers are primarily composed of glucose residues, and their biosynthesis could incorporate the glucose reporter. In previous studies, fucose has been shown to represent the second-highest molar ratio in green seaweed monosaccharide composition, exceeding 20%, in polysaccharides isolated from *Ulva linza* (formerly known as *Enteromorpha linza*) and *Ulva fasciata* (Barakat et al., 2022; Zhang et al., 2013). Ulvan polymers also contain low amounts of galactose, which was also shown to be present within *Ulva* cell wall glycoproteins (Estevez et al., 2009).

The observation in *Ulva* of differences in labelling between the cells present in the same tissue (Fig.5) could be explained by two reasons: (1) cells at different life stages, *e.g*. those that are entering senescence, would integrate the reporter less effectively, and/or (2) due to the seaweed topology; although the surface is superficially relatively flat it may be quite rugged in parts, and this would likely impact the uptake of the label.

The ultrastructure of *Ulva* has already been described. The seaweed is composed of two layers of cells, containing one chloroplast with multiple pyrenoids, a large vacuole and a thick cell wall (Hu et al., 2022; Messyasz et al., 2013). The results of the Lugol staining confirm the presence of starch

inside the seaweed cells, as evidenced by the black-staining spots (Fig. 8e, arrow number 1). In several cells, the nucleus is visualised as larger spots surrounded by a brown membrane (Fig. 8e, arrow number 2)The cell walls are stained light brown due to the presence of ulvans, a major polysaccharide in the cell walls of green seaweed, including *Ulva*.

These results correlate well with the observations made using click chemistry, where strong intracellular labelling was observed, particularly with the glucose reporter (Fig. 5e, j, o). This staining, with iodine, and labelling, with the glucose reporter, is likely to be associated with starch granules. Starch granules are composed of amylose and amylopectins, for which the major monosaccharide component is glucose (Fig.5e, j, o, Supplementary Figure 1l) (Prabhu et al., 2019). However, it can be observed that glucose labelling in starch grains is not as bright as expected. This could be due to a stressful environment for the cells, affecting starch production (Zachleder & Brányiková, 2014).

For the fucose (Fig.5c, h, m) and galactose (Fig.5d, i, n) reporters, we hypothesise that the intracellular labelling observed represents cellular components involved in the synthesis of cell wall sugars, such as the endoplasmic reticulum and the Golgi apparatus. The peripheral localisation of these components could also be explained by variations in osmotic pressure, which might influence their position within the cells. In *Ulva*, punctate fluorescence in the cell walls may be due to localized differences within the cell wall, resulting in the observed fluorescence pattern.

Phycodrys rubens is a perennial red seaweed belonging to the *Delesseriaceae* family, commonly found in the cold, temperate waters of the North Atlantic Ocean (Guiry & Guiry, 2024). It has a flattened, leaf-like thallus (body) that is typically reddish in colour. Its frond has a leafy appearance and is composed of a single flat layer of cells and can grow up to 3 cm wide. Analogues of

galactose, fucose and glucose were incorporated into the cells, and the signals were detected inside the cells or in the cell wall. The labelling of cell walls by the galactose reporter is likely due to carrageenans and agars, which are polysaccharides specific to the cell walls of red seaweed. The galactose reporter may also label galactose-containing glycoproteins in the cell walls. Galactose was previously shown to be present in very high amounts (approximately 90%) among the main neutral sugars identified in soluble dietary fibre from two red seaweed, *Mastocarpus stellatus* and *Gigartina pistillata* (Gómez-Ordóñez et al., 2014).

While fucose is not a major monosaccharide component of red seaweed carbohydrates, several studies have reported its presence in these organisms. For instance, an antioxidant fucose-rich sulphated polysaccharide, additionally containing α-D-Man and β-D-Gal residues, was isolated from the red seaweed *Gloiopeltis tenax* (Lim & Ryu, 2009).

Iodine staining (Lugol reagent) effectively highlighted the presence of floridean starch in *Phycodrys* cells, as evidenced by the dark spots seen at the cell periphery (Fig. 9e, arrow number 1), a feature previously described in the literature (Cole & Sheath, 1990). Similar structures are also visible in the control image (Fig 9.d). Arrow number 2 shows the chloroplast inside the cytoplasm (Fig 9e). The larger oval structures inside the cells (Fig 9e, arrow number 3), which were stained light brown, are likely to be nucleus based on their staining properties (Meyer et al., 2017). The structures observed between cells following staining with Lugol's reagent as well as with TBO (Fig. 9e arrow number 4, arrow f) appear to be the pit plugs, which are characteristic membranous structures specifically found in multicellular red seaweed. Pit plugs are also visible using fucose and galactose reporters in click chemistry Fig. 7i, m, Supplementary Fig 2e (arrow 2). Pit plugs facilitate cell-cell communication but are not considered homologous to

plasmodesmata, which are found in land plants (Pueschel & Cole, 1982). However, despite their different origins, they perform similar roles.

We carried out TBO staining of *Phycodrys*. However, the presence of the red pigments, phycobilins and phycoerythrins, found associated with the chloroplast in many red seaweeds (French & Young, 1952, Gantt et al., 2003), interfered with the visualisation of the stain. The strong red colouration of the pigment made it difficult to distinguish intracellular features that may have stained with toluidine blue from the surrounding background. This limitation highlights the challenges when working with seaweed that contains strong pigments like phycoerythrin, which can mask other cellular details. However, blue-green staining of the cell wall with TBO could clearly be observed as a result of the binding of TBO to carrageenans that are highly sulphated (Gordon-Mills et al., 1978). TBO stains *Ulva* cell walls a different colour because, despite the presence of sulfated groups in ulvans, they contain fewer sulfated groups than carrageenans.

There is a strong correlation between the intracellular components labelled by click chemistry, TBO, and Lugol's reagent. Click chemistry using activated fucose, glucose, and galactose (Fig. 7m, n, o) highlights the presence of unlabeled structures localised at the periphery of the cells. These structures are also observed in the control using only the fluorochrome (Fig 7l). Lugol staining allowed us to identify and confirm that these enigmatic structures are floridean granules. Additionally, click chemistry enabled the labelling of intracellular structures in a nonspecific manner, as these were visible both in the fluorochrome control (Fig. 7l) and with the activated sugars (Fig. 7m, n, o). These structures, similarly observed with Lugol and TBO staining, likely correspond to the seaweed phycobilisomes complex, composed of the phycobiliproteins pigments involved in photosynthesis found in red seaweed (Gantt, 1980). Moreover, some of the intracellular

structures were labelled by all of the activated sugar residues tested (Fig. 7 m, n, o), suggesting that they could be either the location of carrageenans biosynthesis, i.e. within the Golgi apparatus or carrageenans within transport vesicles (Vreeland et al., 1992).

A new experimental approach to characterise cell wall dynamics during seaweed growth

The possibility of incorporating monosaccharide-like chemical reporters into seaweed represents an opportunity to extend physiological and ecological studies of these aquatic species. Uniquely, this approach enables us to measure the potential of organisms to synthesise or modify their cell walls.

Ulva is highly adaptable to various environmental conditions, such as light and temperature fluctuations (Wu et al., 2018). Interestingly, the morphotype of the thalli in *Ulva* may vary in part depending on the water salinity (Rybak, 2018). Indeed, tubular forms present in a very wide range of saline waters, while leaf-shaped thalli are found mainly in brackish waters. Because organ phenotypes are dependent on cell shapes and organisation within tissues, it is clear that approaches using chemical reporters associated with bioorthogonal chemistry will be highly relevant to the study of cell wall dynamics in these seaweeds.

One of the characteristics of Ulvaceae is their ability to produce large amounts of biomass over a short period of time (Rybak & Gąbka, 2018) either in freshwater, even more markedly in seawater, where they are known to be the cause of green tides as in the case for example, in the Yellow Sea off the coasts of Jiangsu and Shandong Province, China (Zhang et al., 2019) or in the English Channel and Atlantic Sea off the coasts of Brittany (Louis et al., 2023). While this proliferation is largely due to an excess of nitrogenous nutrients, cell divisions require massive incorporation of

sugars and, therefore, sustained cell wall material production activities that could be characterised by bioorthogonal click chemistry.

From a biotechnological point of view, the cell walls of seaweed could thus represent a target for better control of their proliferation. To achieve this, it is important to characterise the regulatory elements that enable their construction and then look for inhibitors. Several red seaweeds form blooms and cause premature mortality in marine animals as a result of toxin production (Young et al., 2022). Here, too, knowledge of the wall-forming environment is a prerequisite for finding an effective solution. Additionally, red seaweeds are the primary source of agars and carrageenans, which are polysaccharides widely used as gelling, stabilising, and thickening agents in food, pharmaceuticals, and cosmetics. Their production is largely impacted by the photosynthetic activities of the organisms, but once the monosaccharides have been synthesised, the enzymatic machinery controlling their incorporation in the polymers remains the limiting factor. Bioorthogonal click chemistry can make it possible to select lines that perform better than others in the same way as selection in conventional agriculture.

In summary, we were able to adapt the non-toxic SPAAC click chemistry technique on green and red seaweed. More specifically, we were able to reliably label seaweed cell wall components. Click chemistry is a technique with numerous advantages: it is relatively simple and inexpensive to perform. However, its interpretation is more complex than that of monoclonal antibodies, as the activated sugar can be integrated into various components of the seaweed. While monoclonal antibodies recognize specific epitopes in polymers, their use is more limited. One advantage of click chemistry over antibody staining is its application in cases where polymers are not well-defined (Popper, 2024).

This method opens many avenues of research, including determining changes in seaweed cell walls related to the life cycle and various stresses (grazing, pathogen infection, etc.) that could impact seaweed ecology and diversity, as well as the quality of commercially grown seaweed and the products derived from them.

References cited

Agard, N., Prescher, J., & Bertozzi, C. (2004). A strain-promoted [3 + 2] azide−alkyne cycloaddition for covalent modification of biomolecules in living systems. *Journal of American Chemical Society*, *126*(46), 15046–15047.

Alturkistani, H. A., Tashkandi, F. M., & Mohammedsaleh, Z. M. (2016). Histological stains: A literature review and case study. *Global Journal of Health Science*, *8*(3), 72–79. https://doi.org/10.5539/gjhs.v8n3p72

Anderson, C. T., & Wallace, I. S. (2012). Illuminating the wall: Using click chemistry to image pectins in Arabidopsis cell walls. *Plant Signaling & Behavior*, *7*(6), 661–663. https://doi.org/10.4161/psb.19939

Anderson, C. T., Wallace, I. S., & Somerville, C. R. (2012). Metabolic click-labeling with a fucose analog reveals pectin delivery, architecture, and dynamics in Arabidopsis cell walls. *Proceedings of the National Academy of Sciences*, *109*(4), 1329–1334. https://doi.org/10.1073/pnas.1120429109

Ball, S., Colleoni, C., Cenci, U., Raj, J. N., & Tirtiaux, C. (2011). The evolution of glycogen and starch metabolism in eukaryotes gives molecular clues to understand the establishment of plastid endosymbiosis. *Journal of Experimental Botany*, *62*(6), 1775–1801. https://doi.org/10.1093/jxb/erq411

Barakat, K. M., Ismail, M. M., Abou El Hassayeb, H. E., El Sersy, N. A., & Elshobary, M. E. (2022). Chemical characterization and biological activities of ulvan extracted from *Ulva fasciata* (Chlorophyta). *Rendiconti Lincei. Scienze Fisiche e Naturali*, *33*(4), 829–841. https://doi.org/10.1007/s12210-022-01103-7

Blomme, J., Liu, X., Jacobs, T. B., & Clerck, O. D. (2020). *A molecular toolkit for the green seaweed Ulva mutabilis*. 2020.12.15.422947. https://doi.org/10.1101/2020.12.15.422947

Bothwell, J. H., Goodridge, A. J., Rapin, M., Brennan, P. J., López, A. T., Agrawal, A., Fry, S. C., Campbell, G., & Blomme, J. (2022). *Cell walls are dynamically O-acetylated in the green seaweed,* Ulva compressa (p. 2022.05.24.493306). bioRxiv. https://doi.org/10.1101/2022.05.24.493306

Cardozo, K. H. M., Guaratini, T., Barros, M. P., Falcão, V. R., Tonon, A. P., Lopes, N. P., Campos, S., Torres, M. A., Souza, A. O., Colepicolo, P., & Pinto, E. (2007). Metabolites from algae with economical impact. *Comparative Biochemistry and Physiology. Toxicology & Pharmacology: CBP*, *146*(1–2), 60–78. https://doi.org/10.1016/j.cbpc.2006.05.007

Chalfie M., Tu Y., Euskirchen G., Ward W.W., & Prasher D.C. (1994). Green fluorescent protein as a marker for gene expression. *Science*, *263*(5148), 802–805.

Clarke, A., Anderson, R., & Stone, B. (1979). Form and function of arabinogalactans and arabinogalactan-proteins. *Undefined*. https://www.semanticscholar.org/paper/The-biology-of-arabinogalactan-proteins.-Seifert-Roberts/ee75571a2f49add99a2d6e471c0a36e0a0ba3fcd

Cole, K. M., & Sheath, R. G. (1990). *Biology of the red algae*. Cambridge University Press.

Collén, J., Porcel, B., Carré, W., Ball, S. G., Chaparro, C., Tonon, T., Barbeyron, T., Michel, G., Noel, B., Valentin, K., Elias, M., Artiguenave, F., Arun, A., Aury, J.-M., Barbosa-Neto, J. F., Bothwell, J. H., Bouget, F.-Y., Brillet, L., Cabello-Hurtado, F., … Boyen, C. (2013). Genome structure and metabolic features in the red seaweed *Chondrus crispus* shed light on evolution of the Archaeplastida. *Proceedings of the National Academy of Sciences*, *110*(13), 5247–5252. https://doi.org/10.1073/pnas.1221259110

Coons, A., Creech, H., & Jones, R. (1941). Immunological properties of an antibody containing a fluorescent group. *Experimental Biology and Medecine*, *47*(2), 200–202.

Craigie, J. S. (2011). Seaweed extract stimuli in plant science and agriculture. *Journal of Applied Phycology*, *23*(3), 371–393. https://doi.org/10.1007/s10811-010-9560-4

De Clerck, O., Kao, S.-M., Bogaert, K. A., Blomme, J., Foflonker, F., Kwantes, M., Vancaester, E., Vanderstraeten, L., Aydogdu, E., Boesger, J., Califano, G., Charrier, B., Clewes, R., Del Cortona, A., D'Hondt, S., Fernandez-Pozo, N., Gachon, C. M., Hanikenne, M., Lattermann, L., … Bothwell, J. H. (2018). Insights into the evolution of multicellularity from the sea lettuce genome. *Current Biology*, *28*(18), 2921–2933. https://doi.org/10.1016/j.cub.2018.08.015

Duffieux, D., Marcus, S. E., Knox, J. P., & Hervé, C. (2020). Monoclonal antibodies, carbohydrate-binding modules, and detection of polysaccharides in cell walls from plants and marine algae. In Z. A. Popper (Ed.), *The Plant Cell Wall: Methods and Protocols* (pp. 351–364). Springer. https://doi.org/10.1007/978-1-0716-0621-6_20

Dumont, M., Lehner, A., Vauzeilles, B., Malassis, J., Marchant, A., Smyth, K., Linclau, B., Baron, A., Mas Pons, J., Anderson, C. T., Schapman, D., Galas, L., Mollet, J.-C., & Lerouge, P. (2016). Plant cell wall imaging by metabolic click-mediated labelling of rhamnogalacturonan II using azido 3-deoxy-d-manno-oct-2-ulosonic acid. *The Plant Journal*, *85*(3), 437–447. https://doi.org/10.1111/tpj.13104

Estevez, J. M., Fernández, P. V., Kasulin, L., Dupree, P., & Ciancia, M. (2009). Chemical and in situ characterization of macromolecular components of the cell walls from the green seaweed *Codium fragile*. *Glycobiology*, *19*(3), 212–228. https://doi.org/10.1093/glycob/cwn101

Flint, O. F. (1990). Micro-technique for the identification of food hydrocolloids. *Analyst*, *115*(1), 61–63. https://doi.org/10.1039/AN9901500061

Fournet, I., Deslandes, E., & Floc'h, J.-Y. (1993). Iridescence: A useful criterion to sort gametophytes from sporophytes in the red alga *Chondrus crispus*. *Journal of Applied Phycology*, *5*(5), 535–537. https://doi.org/10.1007/BF02182512

Gantt, E. (1980). Structure and function of phycobilisomes: Light harvesting pigment complexes in red and blue-green algae. In G. H. Bourne, J. F. Danielli, & K. W. Jeon (Eds.), *International Review of Cytology* (Vol. 66, pp. 45–80). Academic Press. https://doi.org/10.1016/S0074-7696(08)61971-3

Gantt, E., Grabowski, B., & Cunningham, F. X. (2003). Antenna systems of red algae: Phycobilisomes with photosystem ll and chlorophyll complexes with photosystem I. In B. R. Green & W. W. Parson (Eds.), *Light-Harvesting Antennas in Photosynthesis* (pp. 307–322). Springer Netherlands. https://doi.org/10.1007/978-94-017-2087-8_10

Gómez-Ordóñez, E., Jiménez-Escrig, A., & Rupérez, P. (2014). Bioactivity of sulfated polysaccharides from the edible red seaweed *Mastocarpus stellatus*. *Bioactive Carbohydrates and Dietary Fibre*, *3*(1), 29–40. https://doi.org/10.1016/j.bcdf.2014.01.002

Gordon-Mills, E. M., Tas, J., & McCandless, E. L. (1978). Carrageenans in the cell walls of *Chondrus crispus* Stack. (Rhodophyceae, Gigartinales).: III. Metachromasia and the topooptical reaction. *Phycologia*, *17*(1), 95–104. https://doi.org/10.2216/i0031-8884-17-1-95.1

Guiry, M. D., & Guiry, G. M. (2024). AlgaeBase. *World-Wide Electronic Publication, University of Galway*.

Hems, E., Wagstaff, B., Saalbach, G., & Field, R. (2018). CuAAC click chemistry for the enhanced detection of novel alkyne-based natural product toxins. *Chemical Communications*, *54*(86), 12234–12237. https://doi.org/10.1039/C8CC05113E

Hu, M., Zhao, S., Liu, J., Tong, Y., Xia, Z., Xia, J., Li, S., Sun, Y., Cao, J., & Zhang, J. (2022). The morphology, genetic diversity, and distribution of *Ulva meridionalis* (Ulvaceae, Chlorophyta) in Chinese seas. *Journal of Marine Science and Engineering*, *10*(12), Article 12. https://doi.org/10.3390/jmse10121873

Huisgen, R. (1961). 1,3-Dipolar cycloaddaitions. *Proceedings of the Chemical Society*, *October*, 357–396. https://doi.org/10.1039/PS9610000357

Ibrahim, W. M. (2011). Biosorption of heavy metal ions from aqueous solution by red macroalgae. *Journal of Hazardous Materials*, *192*(3), 1827–1835. https://doi.org/10.1016/j.jhazmat.2011.07.019

Kloareg, B., & Quatrano, R. S. (1988). Structure of the cell walls of marine algae and ecophysiological functions of the matrix polysaccharides. *Oceanography and Marine Biology*, *26*, 259–315.

Kolb, H. C., Finn, M. G., & Sharpless, K. B. (2001). Click chemistry: Diverse chemical function from a few good reactions. *Angewandte Chemie International Edition*, *40*(11), 2004–2021. https://doi.org/10.1002/1521-3773(20010601)40:11<2004::AID-ANIE2004>3.0.CO;2-5

Lahaye, M. (2001). Developments on gelling algal galactans, their structure and physico-chemistry. *Journal of Applied Phycology*, *13*, 173–184.

Lahaye, M., & Robic, A. (2007). Structure and functional properties of ulvan, a polysaccharide from green seaweeds. *Biomacromolecules*, *8*(6), 1765–1774. https://doi.org/10.1021/bm061185q

Lahaye, M., & Rochas, C. (1991). Chemical structure and physico-chemical properties of agar. *International Workshop on Gelidium*, 137–148. https://doi.org/10.1007/978-94-011-3610-5_13

Leandro, A., Pacheco, D., Cotas, J., Marques, J. C., Pereira, L., & Gonçalves, A. M. M. (2020). Seaweed's bioactive candidate compounds to food industry and global food security. *Life*, *10*(8), Article 8. https://doi.org/10.3390/life10080140

Lion, C., Simon, C., Huss, B., Blervacq, A.-S., Tirot, L., Toybou, D., Spriet, C., Slomianny, C., Guerardel, Y., Hawkins, S., & Biot, C. (2017). BLISS: A bioorthogonal dual-labeling strategy to unravel lignification dynamics in plants. *Cell Chemical Biology*, *24*(3), 326–338. https://doi.org/10.1016/j.chembiol.2017.02.009

Liu, X., Wolfe, R., Welch, L. R., Domozych, D. S., Popper, Z. A., & Showalter, A. M. (2016). Bioinformatic identification and analysis of extensins in the plant kingdom. *PLOS ONE*, *11*(2), e0150177. https://doi.org/10.1371/journal.pone.0150177

Lomartire, S., Marques, J. C., & Gonçalves, A. M. M. (2022). An Overview of the alternative use of seaweeds to produce safe and sustainable bio-packaging. *Applied Sciences*, *12*(6), Article 6. https://doi.org/10.3390/app12063123

Louis, J., Ballu, S., Rossi, N., Lasbleiz, M., Perrot, T., Daniel, C., Cellier, L., Hénaff, F., & Richier, S. (2023). Multi-year renewal of green tides: 18 years of algal mat monitoring (2003–2020) on French coastline (Brittany region). *Marine Pollution Bulletin*, *193*, 115173. https://doi.org/10.1016/j.marpolbul.2023.115173

Makkar, H. P. S., Tran, G., Heuzé, V., Giger-Reverdin, S., Lessire, M., Lebas, F., & Ankers, P. (2016). Seaweeds for livestock diets: A review. *Animal Feed Science and Technology*, *212*, 1–17. https://doi.org/10.1016/j.anifeedsci.2015.09.018

Marketsandmarkets (2023). Algae products market overview 2028. Available at https://www.marketsandmarkets.com/Market-Reports/algae-product-market-250538721.html [accessed 11 June 2024]

Martone, P. T. (2010). Quantifying growth and calcium carbonate deposition of *Calliarthron cheilosporioides* (corallinales, Rhodophyta) in the field using a persistent vital stain. *Journal of Phycology*, *46*(1), 13–17. https://doi.org/10.1111/j.1529-8817.2009.00770.x

Mbua, N. E., Guo, J., Wolfert, M. A., Steet, R., & Boons, G.-J. (2011). Strain-Promoted Alkyne–Azide Cycloadditions (SPAAC) reveal new features of glycoconjugate biosynthesis. *ChemBioChem*, *12*(12), 1912–1921. https://doi.org/10.1002/cbic.201100117

Messyasz, B., Czerwik-Marcinkowska, J., Massalski, A., Uher, B., Rybak, A., Szendzina, L., & Pikosz, M. (2013). Morphological and ultrastructural studies on *Ulva flexuosa subsp. Pilifera* (Chlorophyta) from Poland. *Acta Societatis Botanicorum Poloniae*, *82*(2), Article 2. https://doi.org/10.5586/asbp.2013.013

Meyer, M. T., Whittaker, C., & Griffiths, H. (2017). The algal pyrenoid: Key unanswered questions. *Journal of Experimental Botany*, *68*(14), 3739–3749. https://doi.org/10.1093/jxb/erx178

Minick, M., Fotta, K., & Khan, A. (1991). Polyiodine units in starch–iodine complex: INDO CI study of spectra and comparison with experiments. *Biopolymers*, *31*(1), 57–63. https://doi.org/10.1002/bip.360310106

Morel, O., Lion, C., Neutelings, G., Stefanov, J., Baldacci-Cresp, F., Simon, C., Biot, C., Hawkins, S., & Spriet, C. (2022). REPRISAL: Mapping lignification dynamics using chemistry, data segmentation, and ratiometric analysis. *Plant Physiology*, *188*(2), 816–830. https://doi.org/10.1093/plphys/kiab490

O'Brien, T. P., Feder, N., & McCully, M. E. (1964). Polychromatic staining of plant cell walls by toluidine blue O. *Protoplasma*, *59*(2), 368–373. https://doi.org/10.1007/BF01248568

Pattathil, S., Avci, U., Baldwin, D., Swennes, A. G., McGill, J. A., Popper, Z., Bootten, T., Albert, A., Davis, R. H., Chennareddy, C., Dong, R., O'Shea, B., Rossi, R., Leoff, C., Freshour, G., Narra, R., O'Neil, M., York, W. S., & Hahn, M. G. (2010). A comprehensive toolkit of plant cell wall glycan-directed monoclonal antibodies. *Plant Physiology*, *153*(2), 514–525. https://doi.org/10.1104/pp.109.151985

Pereira, L. (2018). Seaweeds as source of bioactive substances and skin care therapy—Cosmeceuticals, algotheraphy, and thalassotherapy. *Cosmetics*, *5*(4), Article 4. https://doi.org/10.3390/cosmetics5040068

Popper, Z. A. (2024). 13-We all stand together: An exploration of the drivers and constraints that have shaped plant and algal cell wall diversity. In A. Geitmann (Ed.), Plant Cell Wals (1st ed., 275–297). CRC Press.

Popper, Z. A., Michel, G., Hervé, C., Domozych, D. S., Willats, W. G. T., Tuohy, M. G., Kloareg, B., & Stengel, D. B. (2011). Evolution and diversity of plant cell walls: From algae to flowering plants. *Annual Review of Plant Biology*, *62*(1), 567–590. https://doi.org/10.1146/annurev-arplant-042110-103809

Prabhu, M., Chemodanov, A., Gottlieb, R., Kazir, M., Nahor, O., Gozin, M., Israel, A., Livney, Y. D., & Golberg, A. (2019). Starch from the sea: The green macroalga *Ulva ohnoi* as a potential source for sustainable starch production in the marine biorefinery. *Algal Research*, *37*, 215–227. https://doi.org/10.1016/j.algal.2018.11.007

Přerovská, T., Henke, S., Bleha, R., Spiwok, V., Gillarová, S., Yvin, J.-C., Ferrières, V., Nguema-Ona, E., & Lipovová, P. (2021). Arabinogalactan-like glycoproteins from *Ulva lactuca* (Chlorophyta) show unique features compared to land plants AGPs. *Journal of Phycology*, *57*(2), 619–635. https://doi.org/10.1111/jpy.13121

Pueschel, C. M., & Cole, K. M. (1982). Rhodophycean pit plugs: An ultrastructural survey with taxonomic implications. *American Journal of Botany*, *5*(29), 703–720. https://doi.org/10.2307/2442960

Ropitaux, M., Hays, Q., Baron, A., Fourmois, L., Boulogne, I., Vauzeilles, B., Lerouge, P., Mollet, J.-C., & Lehner, A. (2022). Dynamic imaging of cell wall polysaccharides by metabolic click-mediated labeling of pectins in living elongating cells. *The Plant Journal*, *110*(3), 916–924. https://doi.org/10.1111/tpj.15706

Ross, A. G. (1953). Some typical analyses of red seaweeds. *Journal of the Science of Food and Agriculture*, *4*(7), 333–335. https://doi.org/10.1002/jsfa.2740040706

Rybak, A. S. (2018). Species of *Ulva* (Ulvophyceae, Chlorophyta) as indicators of salinity. *Ecological Indicators*, *85*, 253–261. https://doi.org/10.1016/j.ecolind.2017.10.061

Rybak, A. S., & Gąbka, M. (2018). The influence of abiotic factors on the bloom-forming alga *Ulva flexuosa* (Ulvaceae, Chlorophyta): Possibilities for the control of the green tides in freshwater ecosystems. *Journal of Applied Phycology*, *30*(2), 1405–1416. https://doi.org/10.1007/s10811-017-1301-5

Rydahl, M. G., Kracun, S. K., Fangel, J. U., Michel, G., Guillouzo, A., Genicot, S., Mravec, J., Harholt, J., Wilkens, C., Motawia, M. S., Svensson, B., Tranquet, O., Ralet, M.-C., Jorgensen, B., Domozych, D. S., & Willats, W. G. T. (2017). Development of novel monoclonal antibodies against starch and ulvan—Implications for antibody production against polysaccharides with limited immunogenicity. *Scientific Reports*. https://doi.org/10.1038/s41598-017-04307-2

Schindelin, J., Arganda-Carreras, I., Frise, E., Kaynig, V., Longair, M., Pietzsch, T., Preibisch, S., Rueden, C., Saalfeld, S., Schmid, B., Tinevez, J.-Y., White, D. J., Hartenstein, V., Eliceiri, K., Tomancak, P., & Cardona, A. (2012). Fiji: An open-source platform for biological-image analysis. *Nature Methods*, *9*(7), 676–682. https://doi.org/10.1038/nmeth.2019

Schwinn, M. K., Machleidt, T., Zimmerman, K., Eggers, C. T., Dixon, A. S., Hurst, R., Hall, M. P., Encell, L. P., Binkowski, B. F., & Wood, K. V. (2018). CRISPR-mediated tagging of endogenous proteins with a luminescent peptide. *ACS Chemical Biology*, *13*(2), 467–474. https://doi.org/10.1021/acschembio.7b00549

Ścieszka, S., & Klewicka, E. (2019). Algae in food: A general review. *Critical Reviews in Food Science and Nutrition*, *58*(21), 3538–3547.

Sharmila G., Dinesh Kumar, A., Bajhaiya, A. M., Gugulothu, P., & Rajesh, B. (2021). Biofuel production from macroalgae: Present scenario and future scope. *Bioengineered*, *12*(2), 9216–9238. https://doi.org/10.1080/21655979.2021.1996019

Simon, C., Lion, C., Spriet, C., Baldacci-Cresp, F., Hawkins, S., & Biot, C. (2018). One, Two, Three: A bioorthogonal triple labelling strategy for studying the dynamics of plant cell wall formation in vivo. *Angewandte Chemie*, *130*(51), 16907–16913. https://doi.org/10.1002/ange.201808493

Stace, C. A. (1989). *Plant taxonomy and biosystematics*. Cambridge University Press.

Stiger-Pouvreau, V., Bourgougnon, N., & Deslandes, E. (2016). Chapter 8—Carbohydrates from seaweeds. In J. Fleurence & I. Levine (Eds.), *Seaweed in Health and Disease Prevention* (pp. 223–274). Academic Press. https://doi.org/10.1016/B978-0-12-802772-1.00008-7

Subramanian, N., Babu Sreemanthula, J., Balaji, B., R. Kanwar, J., Biswas, J., & Krishnakumar, S. (2014). A strain-promoted alkyne–azide cycloaddition (SPAAC) reaction of a novel EpCAM aptamer–fluorescent conjugate for imaging of cancer cells. *Chemical Communications*, *50*(80), 11810–11813. https://doi.org/10.1039/C4CC02996H

Torode, T. A., Marcus, S. E., Jam, M., Tonon, T., Blackburn, R. S., Hervé, C., & Knox, J. P. (2015). Monoclonal antibodies directed to fucoidan preparations from brown algae. *PLOS ONE*, *10*(2), e0118366. https://doi.org/10.1371/journal.pone.0118366

Torode, T. A., Siméon, A., Marcus, S. E., Jam, M., Le Moigne, M.-A., Duffieux, D., Knox, J. P., & Hervé, C. (2016). Dynamics of cell wall assembly during early embryogenesis in the brown alga Fucus. *Journal of Experimental Botany*, *67*(21), 6089–6100. https://doi.org/10.1093/jxb/erw369

Usov, A. I. (2011). Polysaccharides of the red algae. *Advances in Carbohydrate Chemistry and Biochemistry*, *65*, 115–217. https://doi.org/10.1016/B978-0-12-385520-6.00004-2

Vreeland, V., Zablackis, E., & Laetsch, W. M. (1992). Monoclonal antibodies as molecular markers for the intracellular and cell wall distribution of carrageenan epitopes in Kappaphycus (rhodophyta) during tissue development. *Journal of Phycology*, *28*(3), 328–342. https://doi.org/10.1111/j.0022-3646.1992.00328.x

Wahlström, N., Nylander, F., Malmhäll-Bah, E., Sjövold, K., Edlund, U., Westman, G., & Albers, E. (2020). Composition and structure of cell wall ulvans recovered from *Ulva spp.* Along the Swedish west coast. *Carbohydrate Polymers*, *233*, 115852. https://doi.org/10.1016/j.carbpol.2020.115852

Wichard, T., Charrier, B., Mineur, F., Bothwell, J. H., Clerck, O. D., & Coates, J. C. (2015). The green seaweed Ulva: A model system to study morphogenesis. *Frontiers in Plant Science*, *6*. https://doi.org/10.3389/fpls.2015.00072

Wu, H., Gao, G., Zhong, Z., Li, X., & Xu, J. (2018). Physiological acclimation of the green tidal alga *Ulva prolifera* to a fast-changing environment. *Marine Environmental Research*, *137*, 1–7. https://doi.org/10.1016/j.marenvres.2018.02.018

Young, C. S., Lee, C.-S., Sylvers, L. H., Venkatesan, A. K., & Gobler, C. J. (2022). The invasive red seaweed, *Dasysiphonia japonica,* forms harmful algal blooms: Mortality in early life stage

fish and bivalves and identification of putative toxins. *Harmful Algae*, *118*, 102294. https://doi.org/10.1016/j.hal.2022.102294

Yu, Y., Jia, X., Wang, W., Jin, Y., Liu, W., Wang, D., Mao, Y., Xie, C., & Liu, T. (2021). Floridean starch and floridoside metabolic pathways of *Neoporphyra haitanensis* and their regulatory mechanism under continuous darkness. *Marine Drugs*, *19*(12), 664. https://doi.org/10.3390/md19120664

Yuguchi, Y., Fujiwara, T., Miwa, H., Shirakawa, M., & Yajima, H. (2005). Color formation and gelation of xyloglucan upon addition of iodine solutions. *Macromolecular Rapid Communications*, *26*(16), 1315–1319. https://doi.org/10.1002/marc.200500283

Zachleder, V., & Brányiková, I. (2014). Starch overproduction by means of algae. In R. Bajpai, A. Prokop, & M. Zappi (Eds.), Algal Biorefineries, 217–240. Springer Netherlands. https://doi.org/10.1007/978-94-007-7494-0_9

Zhang, F., Li, Z., Yin, L., Zhang, Q., Askarinam, N., Mundaca-Uribe, R., Tehrani, F., Karshalev, E., Gao, W., Zhang, L., & Wang, J. (2021). ACE2 receptor-modified algae-based microrobot for removal of SARS-CoV-2 in wastewater. *Journal of the American Chemical Society*, *143*(31), 12194–12201. https://doi.org/10.1021/jacs.1c04933

Zhang, L. X., Zhang, N., Li, J., & Wang, Z. (2013). New α-glucosidase inhibitory polysaccharides isolated from marine green algae *Enteromorpha linza*. *Advanced Materials Research*, *634–638*, 1010–1015. https://doi.org/10.4028/www.scientific.net/AMR.634-638.1010

Zhang, Y., He, P., Li, H., Li, G., Liu, J., Jiao, F., Zhang, J., Huo, Y., Shi, X., Su, R., Ye, N., Liu, D., Yu, R., Wang, Z., Zhou, M., & Jiao, N. (2019). *Ulva prolifera* green-tide outbreaks and their environmental impact in the Yellow Sea, China. *National Science Review*, *6*(4), 825–838. https://doi.org/10.1093/nsr/nwz026

Zhao, Q., Nakashima, J., Chen, F., Yin, Y., Fu, C., Yun, J., Shao, H., Wang, X., Wang, Z.-Y., & Dixon, R. A. (2013). LACCASE is necessary and nonredundant with peroxidase for lignin polymerization during vascular development in arabidopsis. *The Plant Cell*, *25*(10), 3976–3987. https://doi.org/10.1105/tpc.113.117770

Acknowledgements

We thank the TisBio and BICeL facilities (University of Lille) for the access to instruments and Thomas Bance for his work on the image capture.

W.F.D. also thanks Clémence SIMON (UGSF-University of Lille) for her support in using Fiji software. This work was supported by a Thomas Crawford Hayes Foundation award to W.F.D.

Additionally, we also wish to thank the Irish Department of Agriculture, Food and Marine (BioCrop) for its financial support under the research stimulus award reference 2019PROG705.

Table Legend

Table 1: Main polysaccharides present in cell walls of different seaweed (adapted from Popper et al. 2011)

	Chlorophyta (green seaweed)	**Rhodophyta (red seaweed)**
Crystalline phase: fiber polysaccharides	Cellulose	Cellulose
Hemicellulose	Xyloglucan Fucan Mannan Glucuronan β-(1→ 3)-glucan	Glucomannan Mannan β-(1→ 3)-glucan β-(1→ 4)-glucan
Amorphous polysaccharides	Ulvan	Agar Carrageenan Porphyran β-(1→ 3)-galactan α-(1→ 3)-glucan

Table 2: Comparison of the signal strength of AF488 for *Ulva spp.* and *Phycodrys rubens* incubated for either a) 24 h or b) 48 h with the reporters for fucose (1,2,3,4-Tetra-*O*-acetyl-6-azido-L-fucopyranose), galactose (1,3,4,6-Tetra-*O*-acetyl-2-azido-2-deoxy-D-galactopyranose), or glucose (1,3,4,6-Tetra-*O*-acetyl-2-azido-2-deoxy-D-glucopyranose) prior to visualisation with DBCO-AF488 and imaging by confocal microscopy.

Conditions	Incubation time	***Ulva spp.***	***Phycodrys ruben***
R-/F+	24 hours	Low signal	Moderate intracellular signal
	48 hours	Low signal	Intracellular significant signal
Fucose/F+	24 hours	Moderate signal, not diffused, labelled cell walls	Intense intracellular signal, slightly labelled cell wall
	48 hours	High signal, diffused, labelled cell walls	Intense intracellular signal
Galactose/F+	24 hours	Moderate signal, diffused, slightly labelled cell walls	Intense intracellular signal, low labelled cell walls
	48 hours	High signal, not too diffused, labelled cell walls	Intense intracellular signal, slightly labelled cell walls
Glucose/F+	24 hours	Moderate signal not diffused, labelled cell walls	Intense intracellular signal, low cell wall signal
	48 hours	High signal, very diffused, intensely labelled cell walls	Intense intracellular signal, slightly labelled cell walls

Figure legends

Figure 1: Photograph of *Ulva spp.* (left) and *Phycodrys rubens* (right), illustrating the two seaweeds studied. Photo taken by W.F.D, Galway, Ireland, October 2023.

Figure 2: Structure of azido activated sugar residues used as reporters of sugar residues present in seaweed cell wall polysaccharides, (a) 1,2,3,4-Tetra-*O*-acetyl-6-azido-L-fucopyranose, (b) 1,3,4,6-Tetra-*O*-acetyl-2-azido-2-deoxy-D-galactopyranose, (c) 1,3,4,6-Tetra-*O*-acetyl-2-azido-2-deoxy-D-glucopyranose. The azide part, shown in blue, can bind with an alkyl part, e.g. shown in Fig. 3, that can be used to visualise the sugars.

Figure 3: Structure of Dibenzocyclooctyne-Alexa Fluor 488 (DBCO-AF488). The AF488 part is shown in green, and the DBCO part is shown in red. The alkyl group, which can bind to the azide group on the modified sugar reporter, is shown in blue.

Figure 4: An illustrated summary of the bioorthogonal labelling strategy used in this work on seaweeds (created using BioRender.com within the agreement number SE27RFKPIS).

Figure 5: Labelling of green seaweed *Ulva spp.* tissues after 48-hour incubation with various reporters. Reporters and fluorochrome: a, f and k, no reporter (R-), no fluorochrome (F-) at x20, x63 and x63x3 (x63 expanded three time) respectively; b, g and l, (R-), with fluorochrome (F+) at x20, x63 and x63x3 (x63 expanded three time) respectively; c, h and m, fucose (R+) (F+) at x20, x63 and x63x3 respectively; d, i and n, galactose (R+) (F+) at x20, x63 and x63x3 respectively; e, j and o, glucose (R+) (F+) at x20, x63 and x63x3 respectively. The arrows indicate the cell walls.

Figure 6: Incorporation of N_3-labelled monosaccharides in red and green seaweed. Reporters were incorporated for 48 hours and detected by the SPAAC reaction. Quantification was carried out by

measuring fluorescence within the cell wall or inside the cell using FIJI, and a comparison was made between fucose, galactose and glucose surrogates. *** Anova test (p-value <0.001).

Figure 7: Labelling of tissues of the red seaweed *Phycodrys rubens* after 48-hour incubation with various reporters. Reporters and fluorochrome: a, f and k, no reporter (R-), no fluorochrome (F-) at x20, x63 and x63x3 (x63 expanded three time) respectively; b, g and l, (R-), with fluorochrome (F+) at x20, x63 and x63x3 (x63 expanded three time) respectively; c, h and m, fucose (R+) (F+) at x20, x63 and x63x3 respectively; d, i and n, galactose (R+) (F+) at x20, x63 and x63x3 respectively; e, j and o, glucose (R+) (F+) at x20, x63 and x63x3 respectively. . The arrows 1 indicate the cell walls, arrows 2 shows the pit-plugs.

Figure 8: Tissues of the green seaweed *Ulva spp.* either unstained or stained with Iodine or Toluidine Blue O. The tissues were unstained and observed at ×40 and ×100 for (a, and d respectively), or stained with iodine- (b, and e) or TBO- (c, and f). Arrow 1 points to starch, and arrow 2 points to a nucleus.

Figure 9: Tissues of the red seaweed *Phycodrys rubens* either unstained or stained with Iodine or Toluidine Blue O. The tissues were unstained and observed at ×40 and ×100 for (a, and d respectively), or stained with iodine- (b, and e) or TBO- (c, and f). Arrow 1 shows the chloroplast and other plastids, arrow 2 shows several chloroplasts, arrow 3 shows the nucleus, and arrow 4 shows the pit plugs.

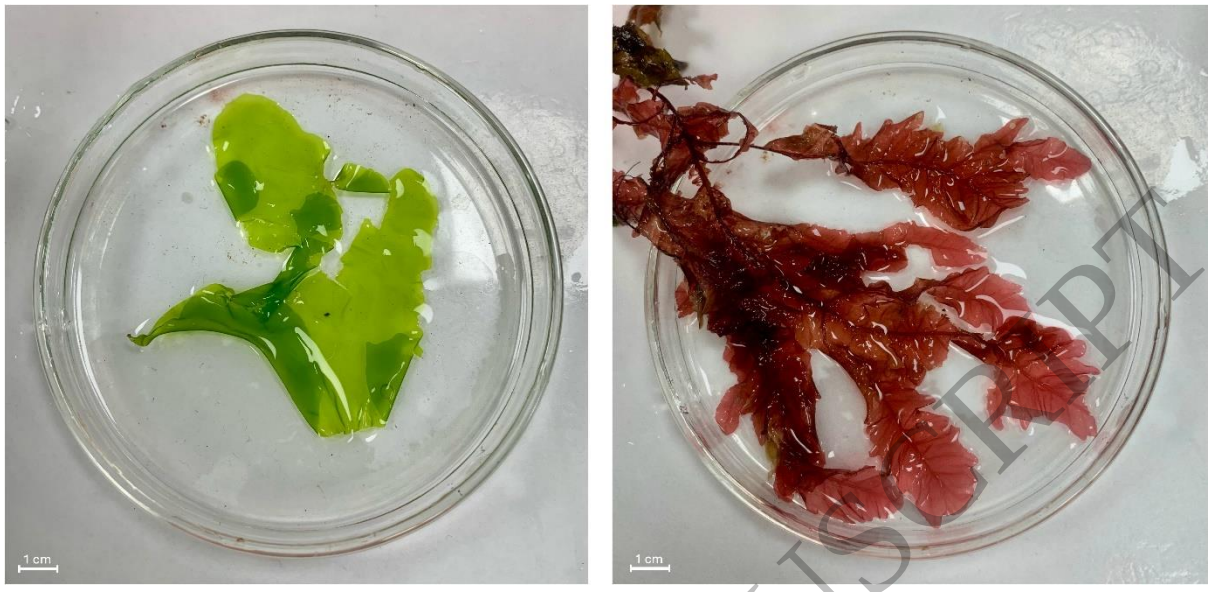

Figure 1
159x77 mm (x DPI)

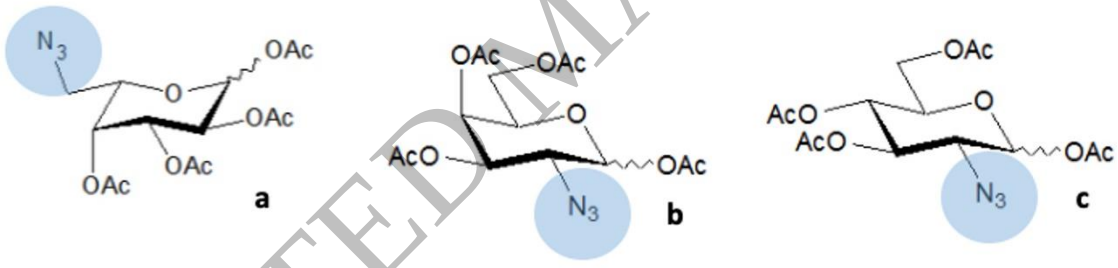

Figure 2
159x43 mm (x DPI)

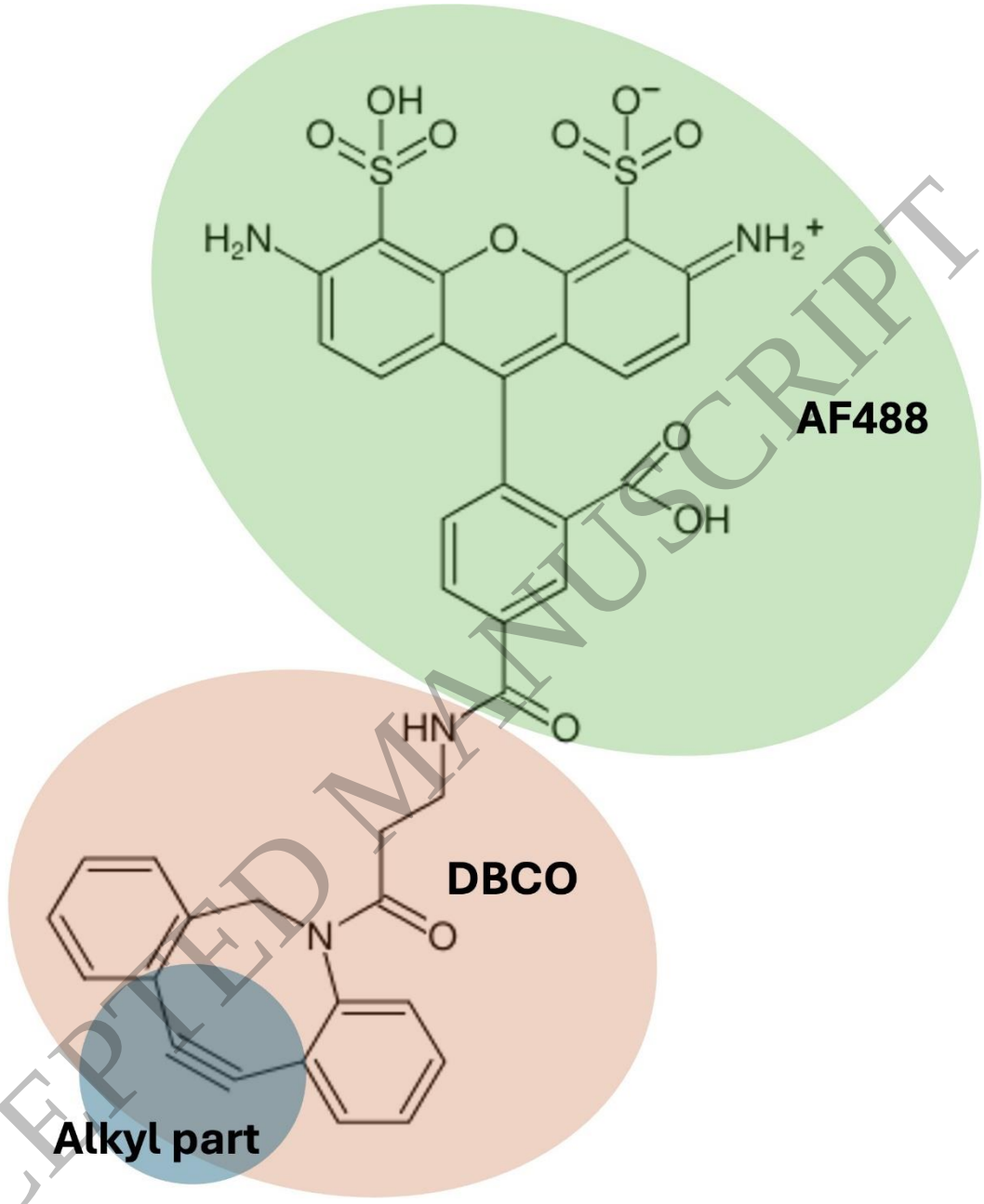

Figure 3
159x170 mm (x DPI)

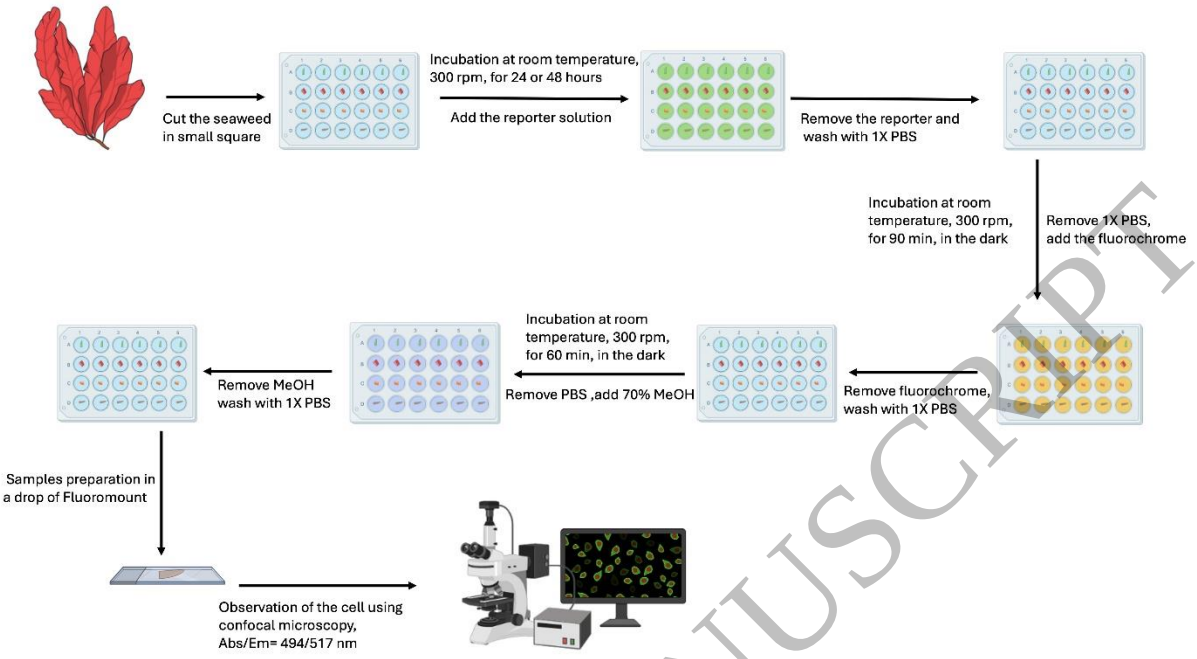

Figure 4
159x88 mm (x DPI)

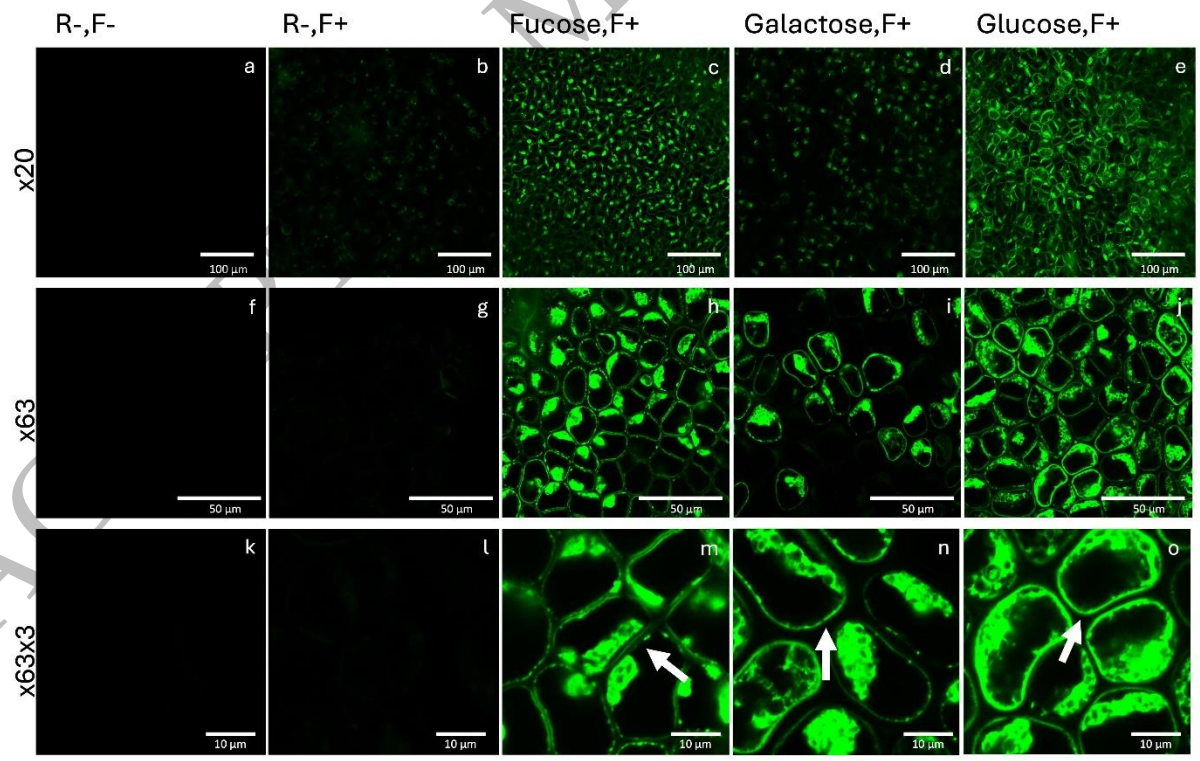

Figure 5
159x104 mm (x DPI)

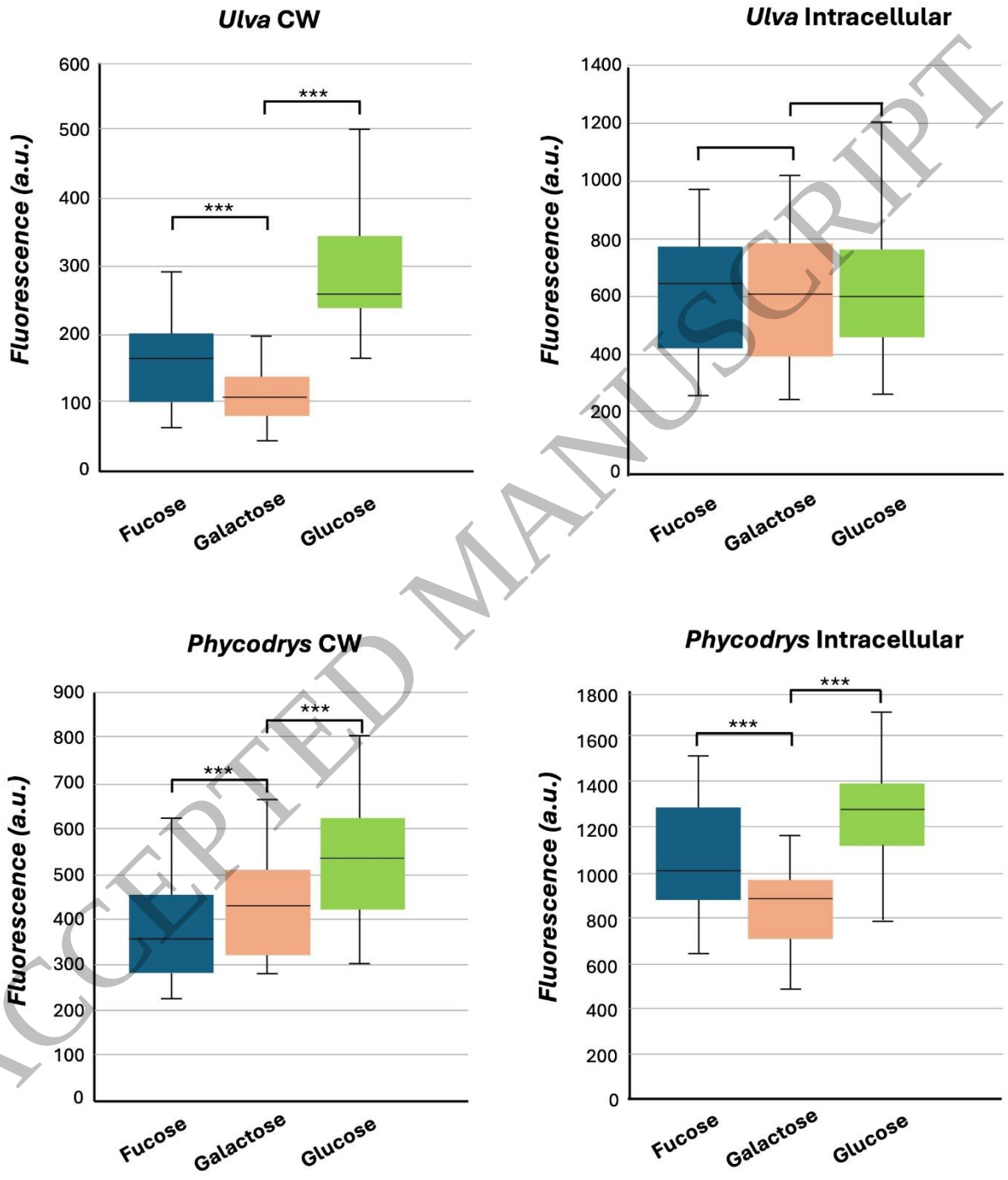

Figure 6
159x200 mm (x DPI)

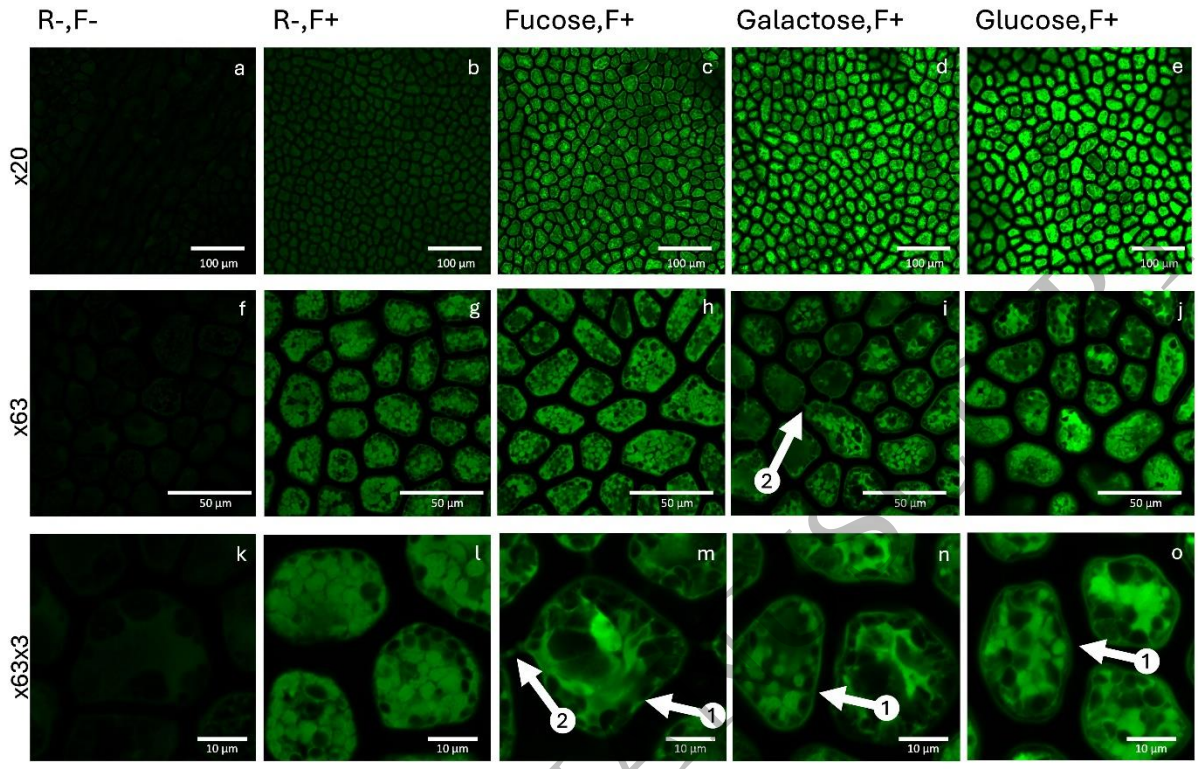

Figure 7
159x105 mm (x DPI)

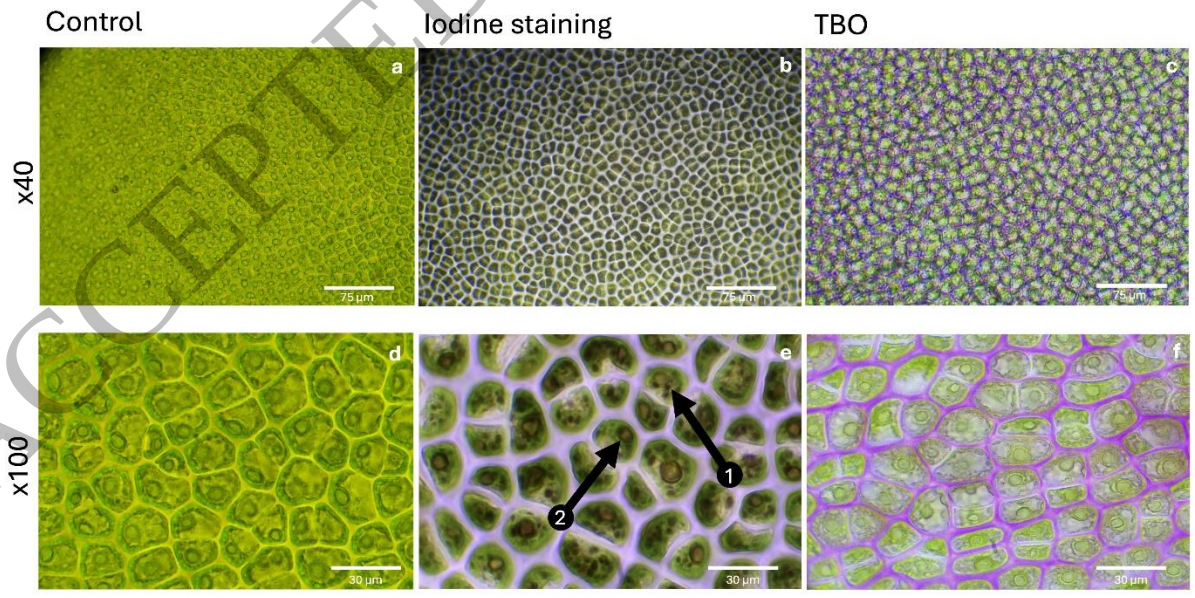

Figure 8
159x80 mm (x DPI)

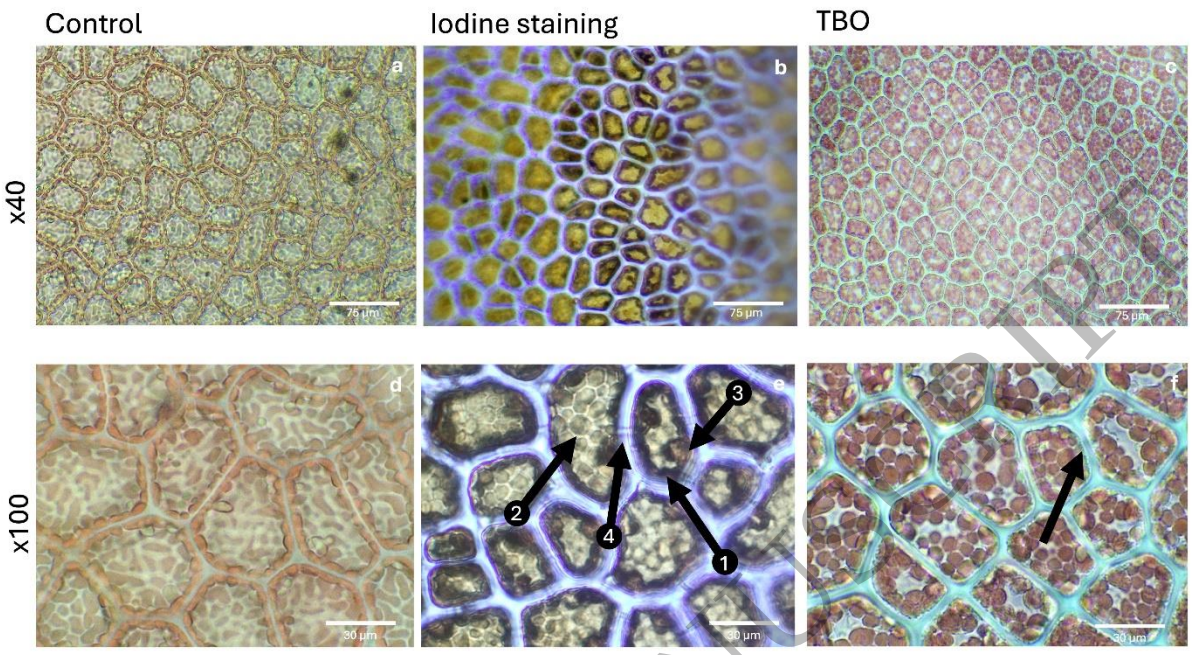

Figure 9
159x87 mm (x DPI)